

# Confirmation of the Luminous Blue Variable status of MWC 930

A. S. Miroshnichenko<sup>1</sup>, N. Manset<sup>2</sup>, S. V. Zharikov<sup>3</sup>, J. Zsargó<sup>4</sup>, J. A. Juárez Jiménez<sup>4</sup>, J. H. Groh<sup>5</sup>, H. Levato<sup>6</sup>, M. Grosso<sup>6</sup>, R. J. Rudy<sup>7</sup>, E. A. Laag<sup>7</sup>, K. B. Crawford<sup>7</sup>, R. C. Puetter<sup>8</sup>, D. E. Reichart<sup>9</sup>, K. M. Ivarsen<sup>9</sup>, J. B. Haislip<sup>9</sup>, M. C. Nysewander<sup>9</sup>, A. P. LaCluyze<sup>9</sup>

<sup>1</sup>Department of Physics and Astronomy, University of North Carolina at Greensboro, Greensboro, NC 27402, USA

<sup>2</sup>CFHT Corporation, 65–1238 Mamalahoa Highway, Kamuela, HI 96743

<sup>3</sup>Instituto de Astronomía, Universidad Nacional Autónoma de México, Apartado Postal 877, 22830, Ensenada, Baja California, México

<sup>4</sup>Departamento de Física, Escuela Superior de Física y Matemáticas del Instituto Politécnico Nacional, Edif. 9, U. P. Zacatenco, 07738, México D. F., México,

<sup>5</sup>Geneva Observatory, Geneva University, Chemin des Maillettes 51, CH–1290 Sauverny, Switzerland

<sup>6</sup>Instituto de Ciencias Astronómicas de la Tierra y del Espacio, CONICET, Casilla de Correo 49, CP 5400, San Juan, Argentina

<sup>7</sup>The Aerospace Corp., M2/266, P.O.Box 92957, Los Angeles, CA 90009, USA

<sup>8</sup>Center for Astrophysics and Space Science, University of California at San Diego, 9500 Gilman Drive, La Jolla, CA 92093, USA

<sup>9</sup>Department of Physics and Astronomy, University of North Carolina, Chapel Hill, NC 27599, USA

**Abstract.** We present spectroscopic and photometric observations of the emission-line star MWC 930 (V446 Sct) during its long-term optical brightening in 2006–2013. Based on our earlier data we suggested that the object has features found in Luminous Blue Variables (LBV), such as a high luminosity ( $\sim 3 \cdot 10^5 L_{\odot}$ ), a low wind terminal velocity ( $\sim 140 \text{ km s}^{-1}$ ), and a tendency to show strong brightness variations ( $\sim 1 \text{ mag}$  over 20 years). For the last  $\sim 7$  years it has been exhibiting a continuous optical and near-IR brightening along with a change of the emission-line spectrum appearance and cooling of the star’s photosphere. We present the object’s  $V$ -band light curve, analyze the spectral variations, and compare the observed properties with those of other recognized Galactic LBVs, such as AG Car and HR Car. Overall we conclude the MWC 930 is a bona fide Galactic LBV that is currently in the middle of an S Dor cycle.

## 1 Introduction

Luminous Blue Variables are evolved massive stars that undergo an evolutionary phase associated with a very strong mass loss. The phase seems to have a short duration [1] that, in combination with a high mass, makes the population of LBVs very small (see [2] for a recent census of Galactic LBVs). Unlike fast winds of most supergiants with terminal velocities of thousands  $\text{km s}^{-1}$ , winds of LBVs are typically slow and dense. These properties in some cases are responsible for formation of circumstellar (CS) dust around LBVs. Other features of LBVs include eruptions on time scales of years when an optical brightening is accompanied by a photospheric cooling and corresponding changes in the ionization state of the CS gas. These variations, which are also called S Dor cycles, along with the wind signatures (narrow spectral lines and rich emission-line spectra) and B–A spectral types allow to identify LBVs almost unambiguously. They are also known to undergo giant eruptions (e.g., P Cyg near 1600 and  $\eta$  Car in 1830’s), but these events are rare and much harder to catch.

In our previous paper [3] we suggested that the emission-line star MWC 930 = V446 Sct is an LBV candidate. Our spectra of the object taken between 2000 and 2004 showed strong and narrow Balmer lines in addition to those of He I and numerous Fe II lines. They also showed absorption lines typically present in luminous stars (e.g., Ne I, N II, and Al III). Combining our photometric data obtained in 1980's and 1990's [4] with those of the ASAS-3 survey (since 1999, [5]), we found that MWC 930 brightened by  $\sim 0.5$  mag in the  $V$ -band in 2004–2005. We followed the object's brightness and spectral variations since that time and now have a firm evidence that the mentioned brightening was an initial stage of a typical S Dor cycle [1].

We describe our observations in Section 2, the observational results are presented in Section 3, modeling of the spectrum is presented in Section 4, the observed behavior of the star and its derived parameters are compared those of other LBVs in Section 5, and conclusions are made in Section 6.

## 2 Observations

Thirty three photometric  $BVRI$  ( $RI$  of the Cousins photometric system) observations were obtained in September 2006 – October 2013 with robotic PROMPT telescopes located in Chile [6]. Transformation equations between the instrumental and standard photometric systems were derived on several nights by taking images of fields that contain standard stars from [7]. The data were reduced with the *daophot* package in IRAF.

Our photometric data were supplemented by  $V$ -band observations from the ASAS-3 survey referred above that currently offers publicly available data until 2011. Individual ASAS-3 data-points that typically come from five separate telescopes were averaged. Since all the stars in our photometric fields are fainter and much bluer than MWC 930, we used the overlapping part of the ASAS-3 light curve to calibrate the  $V$ -band brightness of the object. Only relative variations were measured for the color-indices. A light curve of MWC 930 in the  $V$ -band is shown in Figure 1.

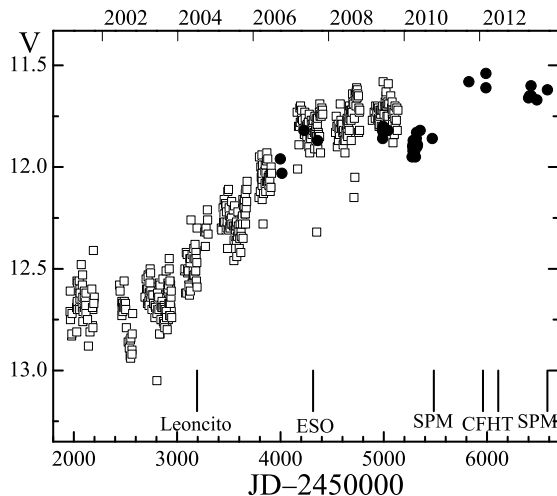


Figure 1:  $V$ -band light curve of MWC 930 in 2001–2013. Open squares show data from ASAS-3, filled circles show our PROMPT data. Short lines show times of the spectral observations and the observatory name. The upper horizontal axis tick marks show beginning time of the indicated years.

Spectroscopic observations were obtained at various observatories in both hemispheres thanks to the object’s nearly equatorial location. Additionally we retrieved a spectrum of the object obtained at the ESO with the spectrograph FEROS and reported in [8]. All the spectra (except the low-resolution one taken at Lick) were obtained with échelle spectrographs. The spectra obtained at the Complejo Astronómico El Leoncito and San Pedro Martir were reduced in a standard way with the *echelle* package in IRAF. Observations obtained at the CFHT were reduced with the Upena and Libre-ESPRIT software packages. The Lick spectrum was absolutely calibrated using a standard star HIP 96379 (G2 v,  $V = 8.83$  mag,  $K = 7.25$  mag). The observing log is presented in Table 1.

Table 1: Spectroscopic observations of MWC 930 in 2004–2013

Date	JD-2450000	Telescope	$R$	Sp.range
2004/07/06 <sup>a</sup>	3193.674	2.1 m Leoncito	15000	4320–6830
2007/08/04	4316.739	2.2 m ESO	48000	4200–8850
2010/10/15	5485.000	2.1 m SPM	15000	4000–6830
2012/02/03	5960.669	3.6 m CFHT	65000	3600–10500
2012/06/29	6107.521	3.6 m CFHT	65000	3600–10500
2013/07/21	6494.898	3.0 m Lick	700	4600–23500
2013/10/17	6583.585	2.1 m SPM	15000	4556–8130

Telescopes and spectrographs used: REOSC at the 2.1 m of the Complejo Astronómico El Leoncito (Argentina), FEROS at the 2.2 m ESO/MPG of the La Silla Observatory (Chile), REOSC at the 2.1 m of the San Pedro Martir (SPM) Observatory (Mexico), ESPaDOns at the 3.6 m CFHT (Hawaii, USA), and NIRI at the 3 m Shane telescope at the Lick Observatory (California, USA).

<sup>a</sup> – the spectrum was reported in [3] and is mentioned here for comparison with the visual maximum data

### 3 Results

In our previous paper [3] we reported that MWC 930 exhibited a stable optical brightness at  $V \sim 12.7 \pm 0.2$  mag in 1989–2003 (we call this period the visual minimum). Since that time the object got  $\sim 1.2$  mag brighter (Fig. 1). The current brightness level with  $V \sim 11.7 \pm 0.2$  mag (since 2007) is called the visual maximum.

Color-indices of MWC 930 changed only slightly during the brightening. In particular,  $B - V$  became  $0.10 \pm 0.05$  mag larger, while  $V - R$  and  $R - I$  remained virtually the same (with a typical scatter of 0.1 mag). The near-IR magnitudes were determined by integration of the absolute fluxes in our Lick spectrum ( $J = 5.7$  mag,  $H = 4.9$  mag,  $K = 4.4$  mag, with an uncertainty of  $\sim 0.1$  mag in all three bands). All the magnitudes are  $\sim 1$  mag brighter than those in the visual minimum [4].

Additionally, MWC 930 was detected in the  $9\text{-}\mu\text{m}$  band by the *AKARI* all sky survey [9] with a flux of  $3.25 \pm 0.02$  Jy. This is  $\sim 0.6$  mag brighter than its MSX flux measured during the visual minimum state [10]. Taking into account that the *AKARI* data were taken in the beginning of the outburst (in 2006–2007) and the object got brighter since then, the relative fluxes of MWC 930 in the range  $0.4\text{--}9\ \mu\text{m}$  changed very little between the visual minimum and maximum.

The high-resolution spectra obtained during the visual maximum show that the spectrum has changed dramatically compared to that observed during the visual minimum. Balmer lines became

somewhat weaker, and the blueshifted emission peak in the  $H\alpha$  line became more pronounced (Beals type III, [11]). Very weak absorption components of the Paschen lines became much stronger, while their emission components got very weak. The number of emission lines increased significantly, while most absorption lines detected earlier became weaker or disappeared. Most weak metallic lines have P Cyg type profiles (a similar description was presented in [12] with no details). The IR calcium triplet lines (8498, 8542, and 8662 Å) show very strong P Cyg type profiles reaching  $\sim 4$  continuum intensities at the peak. The IR oxygen triplet (7772–7775 Å) in absorption, which was present during the visual minimum but not mentioned in [3,8], became stronger. Changes in several regions of the spectrum of MWC 930 between the visual minimum (2001–2004) and maximum (2012) are presented in Fig. 2.

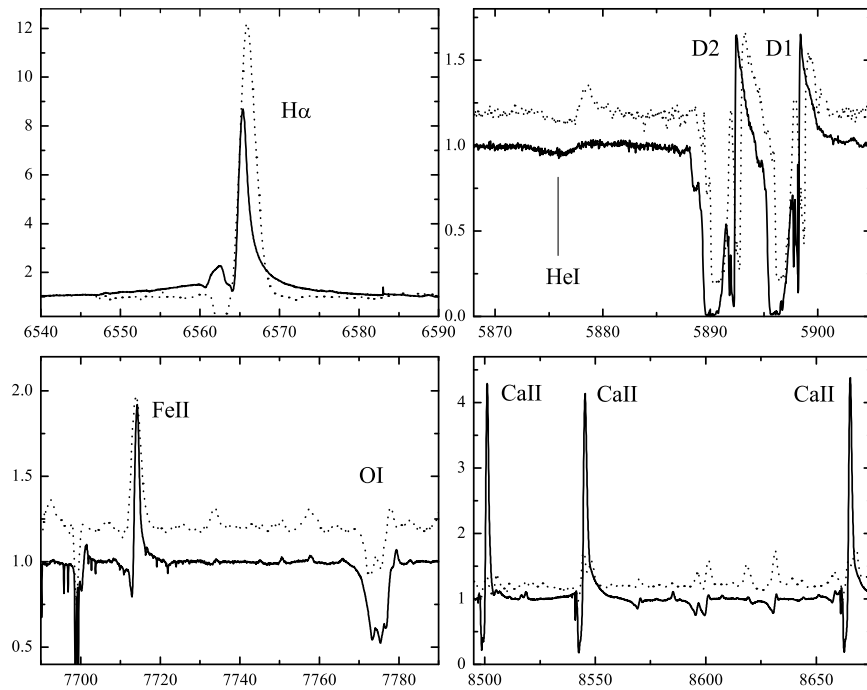


Figure 2: Spectra of MWC 930 obtained at the visual minimum (dotted lines) and maximum (solid lines). The visual minimum spectra were obtained in October 2001 (upper panels) and July 2004 (lower panels). The visual maximum spectrum was obtained in June 2012 (all panels). The intensity is shown normalized to the underlying continuum, and the wavelengths are in Angstroms and heliocentric.

MWC 930 is a relatively optically faint star that also has a very red color ( $B - V \sim 2.5$  mag). Therefore, long exposure times are required even with 2–3 m class telescopes to get a high quality spectrum in the blue wavelength range. Our spectrum obtained at CFHT in June 2012 has a signal-to-noise ratio of  $\geq 30$  in the continuum between 4300 and 5000 Å (and gets to over 100 near  $H\alpha$ ) that allows us to study lines in this spectral region. Parts of it are shown in Fig. 3 for the first time.

All the spectra taken after the beginning of the brightening are very similar to each other. This is not surprising, as they refer to nearly the same brightness ( $V = 11.6$ – $11.8$  mag). Some of their features allow us to evaluate changes in the star’s fundamental parameters compared to those at

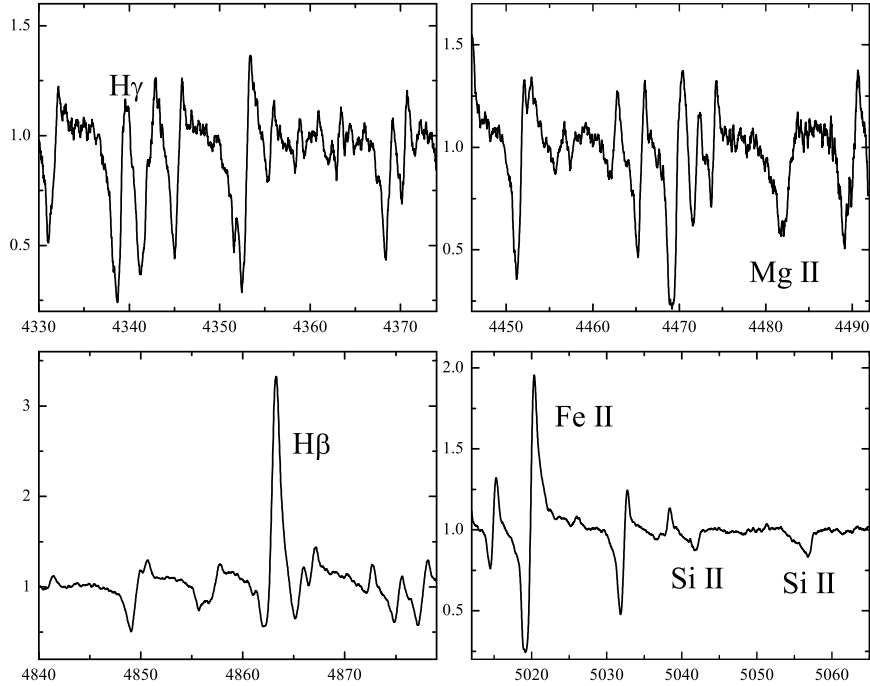


Figure 3: Parts of the CFHT spectrum of MWC 930 obtained on 2012 June 29. The intensity and wavelengths are in the same units as in Fig. 2.

the visual minimum (spectral type B1,  $T_{\text{eff}} = 22000 \pm 5000$  K,  $\log L/L_{\odot} = 5.5 \pm 0.2$ , [3]).

The spectral type during the visual minimum was mainly constrained by the presence of He I lines in emission. These lines are weak and pure in absorption at the visual maximum, indicating a lower effective temperature of the star (see Fig. 2). Another feature is a strong absorption line of Mg II at 4482 Å (Fig. 3). It was reported in [8] as the basis for the object’s spectral classification as B5–B9. The FEROS spectrum used in [8] is very noisy in this wavelength region (signal-to-noise  $S/N \sim 9$  in the continuum) making this conclusion uncertain. Our CFHT spectrum taken in June 2012 has a  $S/N \sim 30$  near the magnesium line and confirms that it is indeed strong and has an equivalent width (EW) of 0.95 Å. It is even stronger than that in spectra of normal supergiants (with no line emission), in which it increases as the effective temperature drops and reaches  $\sim 0.7$  Å at the spectral type F0 (e.g., [13]). This implies that the line is affected by the stellar wind as suggested in [8]. In this case the line EW is not a good indicator of the star’s spectral type.

Nevertheless, we can estimate how cool the photosphere of MWC 930 becomes at the visual maximum. The strength of the emission lines decreases and absorption lines of singly ionized metals get stronger from 2010 to 2013. Comparison with spectra of normal supergiants shows that the absorption-line spectrum resembles those of A5–F0 supergiants (see Fig. 4). Therefore, the star’s effective temperature is around 8000 K.

As the star got cooler, such luminosity indicators as the Si III 5739 Å line [14] that appears in the spectra of early B-type supergiants became unavailable. However, other luminosity criteria can be applied. The EW of the IR oxygen triplet at 7772–7775 Å has been shown to be a reasonably

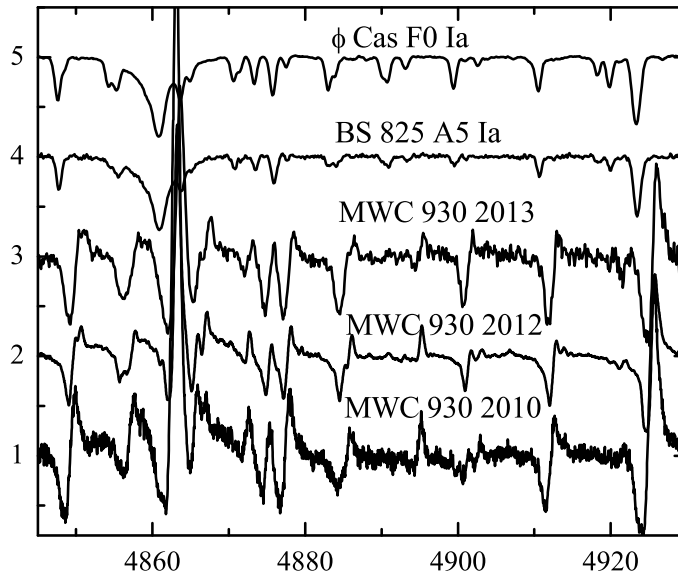


Figure 4: Evolution of the spectrum of MWC 930 in 2010–2013 and comparison with spectra of normal stars. The spectra of BS 825 and  $\phi$  Cas were obtained with a resolving power of  $\sim 10000$  at the Three College Observatory of the University of North Carolina at Greensboro. The intensity and wavelengths are in the same units as in Fig. 2.

good luminosity calibrator in B–F type supergiants (e.g., [15]). The average EW of the triplet in our spectra is  $2.7 \pm 0.1$  Å that corresponds to an absolute visual magnitude of  $M_V \sim -9.0$  mag. The triplet shows a weak emission component on the red side (Fig. 2). Therefore, its properties may be affected by the CS gas and have a limited use. Nevertheless, the triplet EW is very similar (2.8 Å) to that of the A2–hypergiant IRC+10420 (V1302 Aql) which has a bolometric absolute magnitude of  $M_{\text{bol}} \sim -9.5$  mag [16]. Both estimates are within the uncertainty from our earlier result for the object’s luminosity ( $\log L/L_{\odot} = 5.5 \pm 0.2$ , [3]).

Most spectral lines show changes of positions and intensity with time. This is most likely due to a variable mass loss, whose strength affects the density and ionization structure of the stellar wind. Table 2 shows the variability of the H $\alpha$  line profile since our last spectroscopic observation during the visual minimum. The line blue peak and central depression that form in front of the star in an optically-thick part of the wind show significant variations. The red peak that forms in the receding part of the wind shows a stable position, but a variable strength which decreases with time. The latter may be due to a lowering star’s effective temperature and a smaller ionized part of the wind.

The near-IR spectrum of MWC 930 (see Fig. 5) shows significant changes compared to our spectrum obtained in 2001 [3]. The Brackett series hydrogen lines turned into absorption except for Br $_{\gamma}$ . At the same time, a line of neutral sodium at  $2.22 \mu\text{m}$  became stronger. This is also consistent with a lower effective temperature and a smaller ionized part of the wind.

Table 2: Parameters of the H $\alpha$  line in the spectrum of MWC 930 in 2004–2013

Date	Blue		Center		Red		EW, Å
	V <sub>r</sub>	I	V <sub>r</sub>	I	V <sub>r</sub>	I	
2004/07/06 <sup>a</sup>	−94	2.0	−29	0.48	116	18.9	54
2007/08/04	−64	2.2	23	0.73	114	14.5	39
2010/10/15	−6	3.7	49	1.83	118	12.8	36
2012/02/03	+35	2.4	60	1.37	123	8.4	19
2012/06/29	−17	2.2	58	1.20	118	8.8	19
2013/10/17 <sup>b</sup>	−63	1.7	16	0.69	116	8.3	19

Date of observation is listed in column 1; the radial velocity in km s<sup>−1</sup> and the intensity in units of the nearby continuum of the H $\alpha$  line profile parts are listed in columns 2–3 (blue emission peak), 4–5 (central depression), and 6–7 (red emission peak), respectively; column 8 lists the EW of the strongest (red) line peak.

<sup>a</sup> – the spectrum was reported in [3]

<sup>b</sup> – the H $\alpha$  line in this spectrum has an additional absorption component at  $-129$  km s<sup>−1</sup> and 1.11 continuum intensity.

## 4 Modeling

In order to derive stellar wind properties and verify the results of our analysis of the observational data, we used a grid of precalculated models of the radiation transfer code CMFGEN. This code [17] allows for the calculation of non-LTE level populations of the ionization states for all included elements, as well as provides the emergent spectra of the star. It has been used to model spectra of LBVs, O-type and Wolf-Rayet stars [e.g., 18].

Figure 6 shows two fits to a selection of Balmer and He I lines that are reasonably close to the observed line profiles. The weak or nonexistent He I lines indicate a low effective temperature ( $T_{\text{eff}} \leq 10000$  K), and the narrow H $\alpha$  and H $\beta$  suggest a low surface gravity of  $\log g \leq 1$ . It is also obvious from Fig. 6 that the terminal velocity is low ( $v_{\infty} \leq 100$  km s<sup>−1</sup>). Based on these initial constraints, both models were calculated for  $T_{\text{eff}} = 8233$  K and  $\log g = 0.9$ . The spherical stellar wind was described by a  $\beta$  velocity law with  $\beta = 3$  and a terminal velocity of 73 km s<sup>−1</sup> (see [18] for a description of the modeling features). This is consistent with our earlier estimate for the visual minimum state [3].

The mass loss rate was set to be  $\dot{M} = 3 \cdot 10^{-5} M_{\odot} \text{yr}^{-1}$  and  $\dot{M} = 5.6 \cdot 10^{-5} M_{\odot} \text{yr}^{-1}$ . The lower mass loss rate model produces a too weak emission in the H $\alpha$  and H $\beta$ , and the higher mass loss rate model give a too strong emission in these lines.

Since our grid was originally created for modeling AG Car (including elemental abundances adopted from [18]) which has a higher mass loss rate than MWC 930, we can only roughly constrain the mass loss at  $\dot{M} = (4 \pm 1) \cdot 10^{-5} M_{\odot} \text{yr}^{-1}$ . This estimate is over an order of magnitude larger than the one derived for the visual minimum ( $1.5 \cdot 10^{-6} M_{\odot} \text{yr}^{-1}$ ). Such an increase in the mass loss rate during the visual maximum of MWC 930 is larger than that (about a factor of 5) derived for AG Car in [18]. This difference may be due to a lower luminosity of MWC 930. Nevertheless, the effective temperatures of both objects at visual maximum are very close to each other.

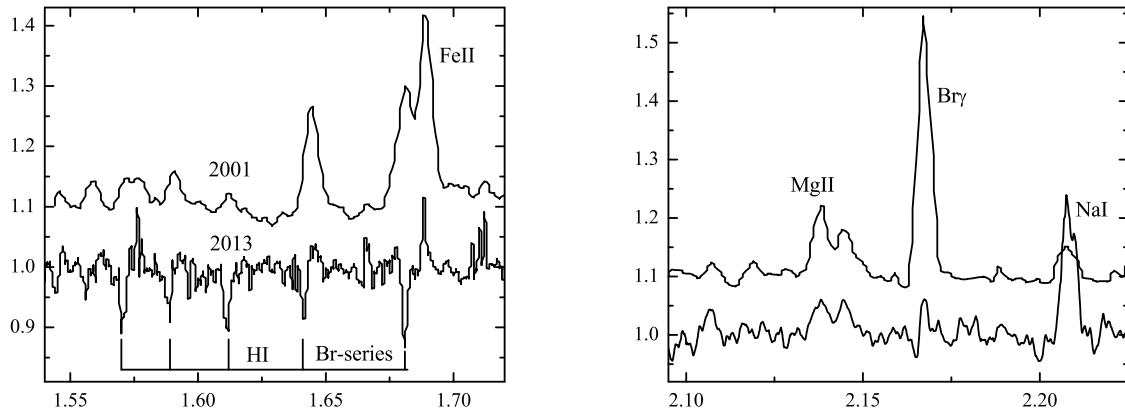


Figure 5: Parts of the Lick near-IR spectrum of MWC 930 obtained on 2013 July 21. The intensity is normalized to the underlying continuum, and the wavelengths are in  $\mu\text{m}$ . The spectrum from 2001 is shifted up by 0.2 continuum intensity.

## 5 Discussion

As we showed above, MWC 930 simultaneously became optically brighter and cooler. This is a typical behavior of an LBV during an S Dor cycle [1]. Therefore the observational data reported here prove our previous suggestion about the nature of this object [3].

The observed behavior can be compared to that of other known LBVs. For example, an S Dor cycle of AG Car that occurred during the 1990's was well documented in [19]. This object began the eruption with a brightness of  $V \sim 8.0$  mag in mid-1990 and reached a maximum brightness of  $V = 5.6$  mag by the end of 1994, then it gradually dimmed to  $V \sim 7.3$  mag by the end of 1998. As it was brightening, its spectrum showed signs of lowering excitation. The following changes were observed in the line profiles between the beginning of the cycle and a brightness level of  $V \sim 6.7$  mag. Lines of neutral helium, which started from P Cyg type profiles with a strong emission component, have disappeared. The Mg II 4482 Å line turned from a weak emission into a strong absorption. Lines of singly ionized iron and titanium had the strongest P Cyg type profiles when the objects was brighter than  $V \sim 6.7$  mag. Qualitatively all these variations were observed during the brightening of MWC 930. The  $H\alpha$  profiles of both AG Car and MWC 930 have a similar structure with a blue peak much weaker than the red one. These similarities strongly suggest that the processes in both objects during the described periods were alike.

While most spectral lines (e.g., Fe II, Ti II) in the spectrum of MWC 930 exhibit pure P Cyg type profiles, the  $H\alpha$  line profile can be described as a combination of a P Cyg type and a double-peaked profile. Such a complicated profile is hard to explain by a spherically-symmetric wind [19]. It needs either an additional disk-like wind component or can be due to a bipolar outflow. Nevertheless, fitting the line's red peak can give an idea about changes of the mass loss rate (see [19] for AG Car). Qualitatively, it appears that the wind becomes stronger with time as the star gets cooler and larger. This process seems to have continued in 2012–2013, as both emission peaks of the  $H\alpha$  line have been getting weaker while the central depression has been getting deeper (see Table 2). The  $H\alpha$  emission peaks are also getting closer together during the visual maximum which is probably an increasing wind optical depth effect.

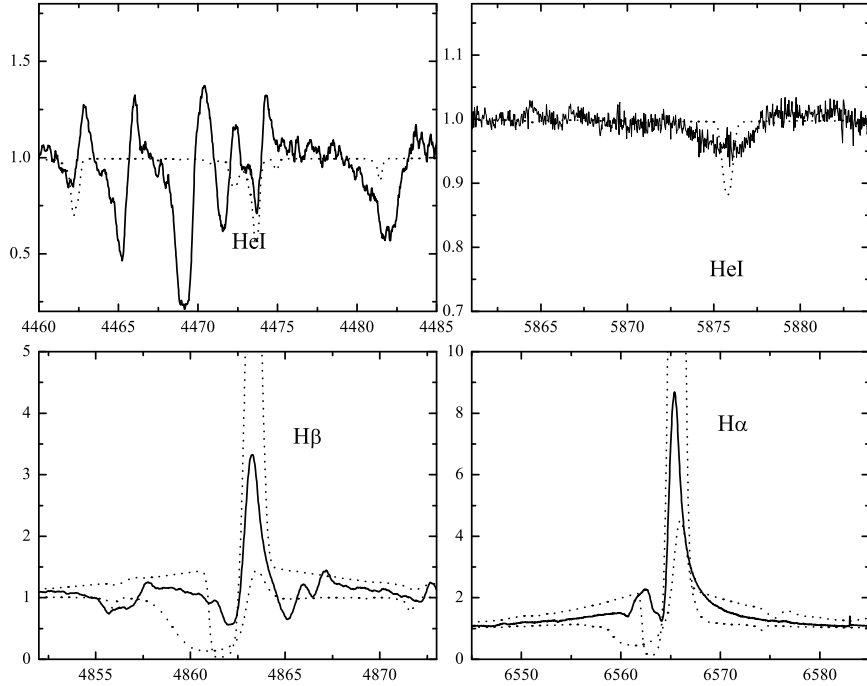


Figure 6: Modeling of selected optical He I lines at 4471 and 5876 Å (upper row), and the H $\alpha$  and H $\beta$  lines (bottom row) for MWC 930. Parts of our CFHT spectrum taken on 2012 June 29 are shown by solid lines, while parts of the model spectra are shown by dotted lines. One model spectrum with a mass loss rate of  $\dot{M} = 3 \cdot 10^{-5} M_{\odot} \text{ yr}^{-1}$  is shown for the He I lines. Two model spectra with mass loss rates of  $\dot{M} = 3 \cdot 10^{-5} M_{\odot} \text{ yr}^{-1}$  (with a weaker line emission) and  $\dot{M} = 5.6 \cdot 10^{-5} M_{\odot} \text{ yr}^{-1}$  are shown for the Balmer lines. The intensity and wavelengths are in the same units as in Fig. 2.

Changes in the LBVs' effective temperature and radius during an S Dor cycle are typically calculated assuming a constant bolometric luminosity [e.g., 19]. This assumption applied to MWC 930 (which is qualitatively supported by the above mentioned luminosity estimates) leads to the following results. Since the object became  $\sim 1.2$  mag brighter in the  $V$ -band (in 2012–2013), then the bolometric correction has got lower by this value. We also need to take into account the CS contribution to the visual continuum which was determined to be  $\Delta V = 0.5$  mag in [3]. We neglect this contribution at the visual maximum, because the ionizing radiation should be much weaker due to a lower effective temperature of the star. If we take  $T_{\text{eff}} = 22000$  K at the visual minimum and a bolometric correction of  $-2.2$  mag [3], then  $T_{\text{eff}}$  is  $\sim 9000$  K for 2012–2013. If  $T_{\text{eff}} = 17000$  K (the lowest value from [3]) that corresponds to a bolometric correction of  $-1.5$  mag [20], then the current  $T_{\text{eff}} \sim 8000$  K. Therefore, we can conclude that MWC 930 has been keeping roughly the same bolometric luminosity during the transition between the visual minimum and maximum.

With these results for the fundamental parameters of MWC 930, one can compare them with those of other LBVs. It has recently been suggested [21] that LBVs which exhibit strong S Dor cycles are fast rotators, and their parameters are constrained by a critical rotation limit. We

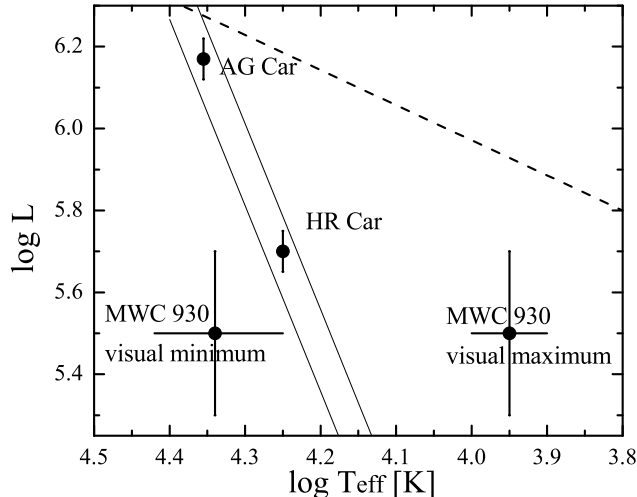


Figure 7: A Hertzsprung-Russell diagram with positions of some LBVs. The solid lines show the boundaries of the visual minimum brightness instability strip for LBVs at which the stellar rotation velocity equals the break-up velocity [20]. The dashed line represents the Humphreys–Davidson stability limit [1]. Fundamental parameters of AG Car and HR Car at a visual minimum are taken from [20]. Luminosity is plotted in the solar units, and temperature in Kelvins.

show the positions of MWC 930 in both brightness states along with those (in a visual minimum state only) of two other strongly variable LBVs, AG Car and HR Car, on the Hertzsprung-Russell diagram in Fig. 7.

The position of MWC 930 during the visual minimum lies in the forbidden area (left of the solid line in Fig. 7) unless we assume the lowest star’s temperature estimated in [3]. The visual maximum position violates no current stability limits. As far as the star’s rotational velocity is concerned, we have suspected in [3] that the broad (and sometimes split) photospheric lines were either due to a fast rotation or binarity. The lower luminosity of MWC 930 compared to those of both AG Car and HR Car is consistent with its weaker emission-line spectrum and therefore a lower mass loss rate.

As we discussed in [3], the presence of a far-IR excess in the spectral energy distribution of MWC 930 was a hint towards the LBV evolutionary status. Recently an extended shell around the object was discovered in IR images taken by the Spitzer Space Observatory and the WISE mission at wavelengths longer than  $5 \mu\text{m}$  [22]. This finding is consistent with the idea of a past giant eruption of MWC 930. Additionally, analysis of the IR spectrum of MWC 930 presented in [22] showed that the silicate absorption feature at  $\lambda = 10\mu\text{m}$  is due to the interstellar rather than to the CS extinction. This result indicates a large distance towards the object and thus supports the high luminosity suggested in [3] and in this paper.

## 6 Conclusions

We reported multicolor optical photometry, high-resolution optical spectroscopy, and low-resolution flux-calibrated near-IR spectroscopy of the LBV candidate MWC 930 obtained in 2006–2013. The observational data clearly show that the object is undergoing an S Dor cycle. During this period the optical brightness increased by  $\sim 1.2$  mag and the spectrum became less excited due to lowering the star’s effective temperature. The spectral features observed at the visual maximum suggest that  $T_{\text{eff}}$  became  $\sim 8000$ – $9000$  K that is consistent with an assumption of the bolometric luminosity constancy during the eruption, as is typically observed in LBVs. Comparison of the spectral behavior and fundamental parameters of MWC 930 with other LBVs that exhibit S Dor cycles (AG Car and HR Car) suggests that the star’s effective temperature during the visual minimum was on the lowest side of our previous estimate ( $\sim 17000$  K, [3]), while the bolometric luminosity ( $\log L/L_{\odot} \sim 5.5$ , [3]) did not seem to change.

## 7 Acknowledgements

We are grateful to M. Borges Fernandes for retrieving and reducing the FEROS spectrum of MWC 930. A. M. and S.Z. acknowledge support from DGAPA/PAPIIT project IN100614. This paper is partially based on observations obtained at the Canada-France-Hawaii Telescope (CFHT) which is operated by the National Research Council of Canada, the Institut National des Sciences de l’Univers of the Centre National de la Recherche Scientifique de France, and the University of Hawaii, the 2.2m MPG telescope operated at ESO/La Silla under program IDs 086.A–9019 and 087.A–9005, the 2.1m telescope of the San Pedro Martir Observatory, the 2.1m telescope of the Complejo Astronómico El Leoncito, and the PROMPT robotic telescopes located in Chile and operated by University of North Carolina at Chapel Hill.

### References:

1. R. M. Humphreys, K. Davidson, “The luminous blue variables: Astrophysical geysers”, *Publications of the Astronomical Society of the Pacific*, vol. 106, pp. 1025–1051, 1994.
2. J. S. Clark, V. .M. Larionov, A. A. Arkharov, “On the population of galactic Luminous Blue Variables”, *Astronomy and Astrophysics*, vol. 435, pp. 239–246, 2005.
3. A. S. Miroshnichenko, K. S. Bjorkman, M. Grosso, et al., “MWC 930 - a new luminous blue variable candidate”, *Monthly Notices of the Royal Astronomical Society*, vol. 364, pp. 335–343, 2005.
4. Yu. K. Bergner, A. S. Miroshnichenko, R. V. Yudin, et al., “Observations of emission-line stars with IR excesses. II. Multicolor photometry of B[e] stars.”, *Astronomy and Astrophysics Supplement Series*, vol. 112, pp. 221–228, 1995.
5. G. Pojmanski, “The All Sky Automated Survey. Catalog of Variable Stars. I. 0 h – 6 h Quarter of the Southern Hemisphere”, *Acta Astronomica*, vol. 52, pp. 397–427, 2002.
6. D. E. Reichart, M. Nysewander, J. Moran, et al., “PROMPT: Panchromatic Robotic Optical Monitoring and Polarimetry Telescopes”, *Nuovo Cimento C*, vol. 28, pp. 767–770, 2005.
7. A. U. Landolt, “UBVRI photometric standard stars around the celestial equator”, *Astronomical Journal*, vol. 88, pp. 439–460, 1983.
8. A. Carmona, M. E. van den Ancker, M. Audard, et al., “New Herbig Ae/Be stars confirmed via high-resolution optical spectroscopy”, *Astronomy and Astrophysics*, vol. 517, A67, 22 pp., 2010.

9. D. Ishihara, T. Onaka, H. Kataza, et al., “The AKARI/IRC mid-infrared all-sky survey”, *Astronomy and Astrophysics*, vol. 514, A1, 14 pp., 2010.
10. M. P. Egan, S. D. Price, K. E. Kraemer, et al., “The Midcourse Space Experiment Point Source Catalog Version 2.3 (October 2003)”, AFRL-VS-TR-2003-1589, 2003.
11. C. S. Beals, “The Spectra of the P Cygni Stars”, *Publications of the Dominion Astrophysical Observatory*, vol. 9, pp. 1–49, 1953.
12. A. Lobel, J. H. Groh, K. Torres, N. Gorlova, “Long-term spectroscopic monitoring of LBVs and LBV candidates”, in *Active OB stars: structure, evolution, mass loss, and critical limits*, Proceedings of the Symposium, Vol. 272, pp. 519–520, 2011.
13. D. J. Lennon, P. L. Dufton, A. Fitzsimmons, “Galactic B-supergiants. II. Line strengths in the visible – Evidence for evolutionary effects?”, *Astronomy and Astrophysics Suppl. Ser.*, vol. 97, pp. 559–585, 1993.
14. A. S. Miroshnichenko, H. Levato, K. S. Bjorkman, et al. 2004. “Properties of Galactic B[e] supergiants. III. MWC 300”, *Astronomy and Astrophysics*, vol. 417, pp. 731–743, 2004.
15. V. V. Kovtyukh, N. I. Gorlova, S. I. Belik, “Accurate luminosities from the oxygen 7771–4 Å triplet and the fundamental parameters of F–G supergiants”, *Monthly Notices of the Royal Astronomical Society*, vol. 423, pp. 3268–3273, 2012.
16. V. G. Klochkova, M. V. Yushkin, E. L. Chentsov, V. E. Panchuk, “Evolutionary Changes in the Optical Spectrum of the Peculiar Supergiant IRC+10420”, *Astronomy Reports*, vol. 46, pp. 139–152, 2002.
17. D. J. Hillier, D. L. Miller, “The Treatment of Non-LTE Line Blanketing in Spherically Expanding Outflows”, *Astrophysical Journal*, vol. 496, pp. 407–427, 1998.
18. J. H. Groh, D. J. Hillier, A. Damineli, et al., “On the Nature of the Prototype Luminous Blue Variable AG Carinae. I. Fundamental Parameters During Visual Minimum Phases and Changes in the Bolometric Luminosity During the S–Dor Cycle”, *Astrophysical Journal*, vol. 698, pp. 1698–1720, 2009.
19. O. Stahl, I. Jankovics, J. Kovács, et al., “Long-term spectroscopic monitoring of the Luminous Blue Variable AG Carinae”, *Astronomy and Astrophysics*, vol. 375, pp. 54–69, 2001.
20. A. S. Miroshnichenko, “New photometric calibration of the visual surface brightness method”, in *Fundamental Stellar Properties: The Interaction between Observation and Theory*, Proc. IAU Symp. 189, pp. 50–53, 1997.
21. J. H. Groh, A. Damineli, D. J. Hillier, et al., “Bona Fide, Strong-Variable Galactic Luminous Blue Variable Stars are Fast Rotators: Detection of a High Rotational Velocity in HR Carinae”, *Astrophysical Journal*, vol. 705, pp. L25–L30, 2009.
22. L. Cerrigone, G. Umana, C. S. Buemi, et al., “Spitzer observations of a circumstellar nebula around the candidate Luminous Blue Variable MWC 930”, *Astronomy and Astrophysics*, vol. 562, A93, 9 pp., 2014.